



Computational drug design targeting MYH7 for hypertrophic cardiomyopathy integrating molecular docking, Density Functional Theory, and Molecular Dynamics Simulations

Nimra Hanif^{1*}, Amina Arif¹, Sadia Ali¹, Muqddas Anees², Mavra Anees¹, Arooj Arshad¹, and Muhammad Asim¹

¹University of Central Punjab, Faculty of Science and Technology, Department of Biotechnology, Lahore, Pakistan

²University of Central Punjab, Faculty of Science and Technology, Department of Microbiology, Lahore, Pakistan

*Correspondence:

Nimra Hanif

Email: hnimra426@gmail.com

Received: March 23, 2025

Revised: July 15, 2025

Accepted: August 29, 2025

ABSTRACT: Hypertrophic cardiomyopathy (HCM) is a genetic condition of the heart that is commonly associated with mutations of sarcomeric proteins such as MYH7. Currently available therapies are largely palliative and do not offer cure-focused treatment. In this work, we utilize a computational approach combining molecular docking, Density Functional Theory (DFT), and Molecular Dynamics (MD) simulations to search for therapeutic compounds interacting with the MYH7 protein. Predicted models of MYH7 by Alpha Fold provided strong prediction reliability since 91.4% of residues were in the favored Ramachandran region. Out of multiple bioactive candidates screened, thymoquinone showed the most negative free energy of binding (-6.7 kcal/mol) to MYH7. Pharmacophore modeling along with ADMET analysis also validated its druglike nature and declared safety. Analyzing electronic properties showed that thymoquinone possesses a low HOMO-LUMO band gap (~5.67 eV), thus showcasing strong bioreactivity and stability. These results provide a direction for the intervention of MYH7 protein dysfunction. Such progress would aim at changing the treatments from palliative strategies to curative approach which is particularly essential to mitigate the risk of sudden cardiac death, especially in children. However further in vitro and in vivo studies are required to validate the safety and efficiency of the thymoquinone.

KEYWORDS: Hypertrophic Cardiomyopathy (HCM), Left Ventricular Hypertrophy, Myocardial Ischemia, MYH7 Gene, MYBPC3 Gene, and Pharmacophore Modeling.

INTRODUCTION

Hypertrophic cardiomyopathy (HCM) is a genetic cardiovascular disease characterized by left ventricular hypertrophy, diastolic dysfunction, myocardial ischemia, and severe complications, such as arrhythmias and sudden cardiac death (SCD) [1]. It has an estimated prevalence of approximately 0.2% and is considered to be fairly rare. However, it is the second most common cause of cardiomyopathy of children in Brazil [2]. In 2010, there was an 18.31% increase in the mortality rate from cardiovascular causes (unilateral effect, non-homotoxic events) among 68,000 white males aged 40 years and older in Brazil. However, management of HCM has seen significant improvement over the last two decades and although disease-modifying therapies for HCM have been developed such as disopyramide and calcium channel blockers, they are limited in efficacy [3].

There is now a growing interest in precision medicine strategies as a method of intervention and prevention for

health care systems to address the different genetic diversity and progression of HCM [4].

It is caused by mutations in the sarcomeric protein genes MYH7 and MYBPC3, which have greater than 70% of cases. More than 200 MYH7 mutations are associated with adverse outcome, including Arg403Gln and Arg719Trp; however, other clinical variables can influence prognosis. In silico experiments show that specific mutations, such as MYH7 G256E, increase hypercontractility and mitochondrial activity; these findings provide insight into the interaction of genotype and phenotype [5]. Although prevalence is 0.2% it is still underdiagnosed because the disease sufferers exhibit subtle symptoms. Improvements in genetic research and imaging of HCM have improved diagnosis and management [6].

Hypertrophic cardiomyopathy is a genetic cardiac disease including diastolic dysfunction, arrhythmias, and sudden cardiac death [7]. It has a prevalence of 0.2% but is still poorly understood due to subtle manifestations, as well

as variability in presentation. HCM is caused mainly by mutations in the genes encoding sarcomere proteins, MYH7 and MYBPC3 [8]. Diagnostic criteria include echocardiography or magnetic resonance imaging to evaluate abnormal wall thickness, which could be achieved using one of the available imaging techniques: echocardiography or MRI [9]. The introduction of genetic testing has been helpful in early detection and risk stratification but still present challenges in predicting outcome due to phenotypic variability [10].

Hypertrophic cardiomyopathy is a common inherited heart condition affecting about 1 in 500 adults worldwide [11]. It can be diagnosed by echocardiography of the left ventricular wall. This condition may cause dysfunction of the diastolic function of the cardiac valve as well as cardiac arrhythmias and even death of the heart as a result [12]. Hypertrophic cardiomyopathy has a high recurrence rate but largely unsuspected and requires reintroduction of screening, especially in at-risk adults [13].

HCM is diagnosed through echocardiography, but genetic testing is used to screen individuals at higher risk [14]. The expression of the genes associated with HCM has differed greatly, and thus it does not have a strong predictive power. Advances in genetic research have improved our understanding of the molecular basis of HCM, and now gene-based diagnostic methods can be used more effectively which can lead to early recognition and targeted treatment [15]. Clinical presentations differ widely, from relatively symptomatic and non-disruptive conditions to severe heart failure. Given that one of the most challenging aspects of managing HCM is identifying and correcting the cause of the disease, the identification and management of patients who were previously thought not to have HCM should continue to be explored and appropriate management strategies developed [16].

AI technology has revolutionized pharmaceutical research by automating the identification of key drug targets and optimizing leads through the enhancement of various developmental processes. The application of ML and DL algorithms enables virtual screening of compounds through rapid evaluation of extensive chemical libraries, streamlining the identification of candidates for drug development. These AI-driven models predict molecular properties such as solubility, permeability, and toxicity, crucial for assessing drug-likeness and safety profiles [17]. Moreover, Alpha Fold can predict protein structures with unparalleled precision which facilitates structure-based drug design [18]. Implemented AI models synergistically boost the speed of executing tasks, which improves their precision and efficacy,

fundamentally improving the quality of pharmaceutical research.

MATERIALS AND METHODS

Retrieval of targeted protein

Primary sequence of targeted protein MYH7 was retrieved by utilizing an online bioinformatics database NCBI (National Center of Biotechnology Information) [19].

Physicochemical Analysis

ExPasy ProtParam is an online tool that was used to predict physicochemical properties of MYH7 that results in different analysis including amino acids residues numbers, molecular weight protein nature, and stability [20].

Tertiary Structure Prediction

Tertiary structure of MYH7 protein predicted by AlphaFold3 structure database an AI tool that used deep learning algorithms to predict the 3D structure of protein including protein evolution and structural conservation and provide 90-95% accurate structures that is developed by DeepMind and EMBL-EBI [21].

Tertiary structure validation

Validated the 3D alphafold structure of MYH7 protein by using Ramachandran plot that revealed the procheck results indicating torsion angle distribution thereby confirming the structural reliability of the protein. A well-validated 3D structure exhibit significant percentage of residues in the most favored region with minimal or no residues located in disallowed regions [22].

Identification of the ligands

There are several bioactive compounds were selected as potential ligands, including Genistein, Thymoquinone, Gingerol, Quercetin, Resveratrol, Vanillin and Allyl isothiocyanate were selected from literature for in silico drug screening approach targeting MYH7 protein. 3D structure of these compounds were obtained in SDF format from PubChem [23].

Molecular Docking

Molecular docking was performed by using multi-ligand docking tool named as PyRx of all compounds Thymoquinone, Curcumin, Epigallocatechin Gallate, Gingerol, Quercetin, Resveratrol, and vanillin at once designed for computational drug discovery to check the molecular interaction energies between targeted protein and ligands molecules. Furthermore interaction analysis was

performed by using the Discovery studio tool to predict the active binding residues of protein and bond interactions [24].

Pharmacophore characterization

The Pharmit tool was utilized for pharmacophore modeling and virtual screening, enabling the identification of key interaction points between ligands and their target receptors. Pharmacophore modeling, a foundational concept in virtual screening introduced in drug discovery workflows, enables the identification of key structural features responsible for biological activity [25]. It was used for the generation of pharmacophore models based on the three-dimensional structures of proteins [26].

ADMET analysis

The SwissADME tool was utilized for the preclinical evaluation of a drug candidate, providing properties i.e absorption, skin permeability, bioavailability score and molar refractivity. Additionally, the toxicity profile of the ligand was evaluated through the ProTox II server which offers insights into potential adverse effects [27].

Density functional theory Analysis

In order to determine the bioreactivity of the ligand, Density functional Theory analysis was done through the use of Gauss view and Gaussian 09W tools. Density Functional Theory (DFT), originally developed by Parr and Yang (1989), offers a reliable method for predicting electronic structures of molecules and has been widely applied in computational drug discovery [28]. The DFT method was employed at the ground state, with default spin, B3YLP and basis set of 6-31G with singlet spin. Result summary, Highly occupied molecular orbital energy (HOMO) and Lowest unoccupied molecular orbital energy (LUMO) was noted and Band gap energy was determined to elucidate the bioreactivity of the ligand [29].

Molecular Interaction analysis

PyRx an offline multi docking software utilized for docking analyses of selected active compounds with the MYH7 protein. Following this setup, eight ligand conformations were produced, and the most favorable conformation was chosen for detailed molecular interaction studies, which were visualized using Bio-discovery Studio, resulting in both 3D and 2D interaction diagrams. The docking grid box was configured with center coordinates X = -10.207, Y = 7.270, Z = 13.300 and dimensions 25.00 Å × 25.00 Å × 25.00 Å with exhaustiveness values of 8, ensuring complete coverage of the active binding site of the MYH7 protein [30].

Molecular dynamic simulation

The IMOD tool was utilized to perform simulations of MYH7- Thymoquinone docking complex, allowing for the analysis of protein dynamics and structural flexibility. These analyses contributed to a comprehensive understanding of the protein's dynamic behavior during the simulation [31].

RESULTS

Primary sequence and physiochemical analysis

NCBI was used to retrieve the primary sequence of MYH7 protein in FASTA format by the accession number (NP_001393933). ExPasy ProtParam predicted physiochemical properties of MYH7 protein showing the hydrophilic nature of protein by the highest negative charged residues (358) as compared to positive charged residues (316) with total number of 1935 amino acid residues, molecular weight 223097.30, having instability effect 47.05 and aliphatic index 82.19.

Retrivel of the tertiary structure

The 3D structure of the MYH7 protein in Homo sapiens was predicted using AlphaFold through a series of computational processes enhancing the accuracy of the final model. Reliability scores were calculated for various regions of the predicted structure, indicating the confidence in these predictions and providing a detailed model for further research into the protein's biological functions. Very highest confidence value is greater than 90, highest confidence value is 70 shows in light blue or green color, while lowest value rang is 50 that shows in brown color that is visible in protein 3D structure. Here is the 3D structure of AlphaFold MYH7 protein below in Figure 1.

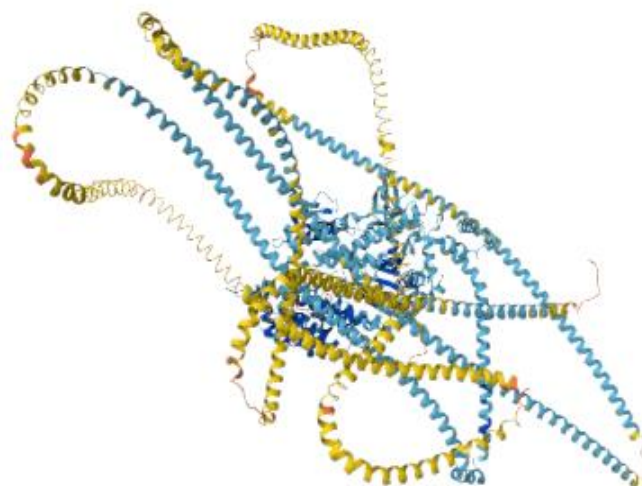


Figure 1. MYH7 protein 3D structure

Tertiary structure validation

The Ramachandran plot was generated to evaluate the conformational quality of the protein, with total 1935 protein residues, where 91.4% of the analyzed 160 amino acid residues were located within the favored and most favored regions, 0.2% residues were located within disallowed region while 0.3% were located within generally allowed region. This high percentage indicates that the protein adopts stable and energetically favorable conformations. The detailed representation of dihedral angles (ϕ and ψ) in the plot can be observed in Figure 2. Phi (ϕ) angle is indicating the movement between Nitrogen atom and Carbon atom while psi (ψ) indicates the movement between central carbon and carbon atom of carboxylic of other amino acid.

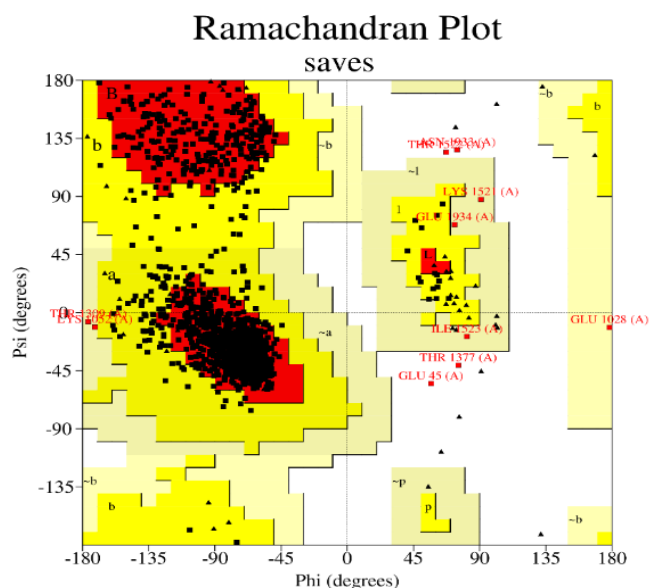


Figure 2. Ramachandran plot of MYH7 alpha fold protein

Identification of ligands

For screening purposes, Genistein, Thymoquinone, Gingerol, Quercetin, Resveratrol, Vanillin and were selected from the literature as indicated that have potential to become drug candidate targeting MYH7-protein for treating cardiovascular disease. The 3D structures of these compounds were retrieved from PubChem in SDF format. Subsequently, the SDF files were converted to PDB format using Discovery Studio to facilitate further analysis. Here is the table.1 of phytochemicals used.

Molecular docking

The docking results for the eight ligands i.e Thymoquinone, Curcumin, Epigallocatechin Gallate, Gingerol, Quercetin, Resveratrol, and vanillin were obtained using PyRx multiple protein-ligand docking tool. Each ligand

was docked against the target protein MYH7 alpha fold and their binding affinities were calculated. The binding affinities revealed significant variations among the ligands, with values indicating their potential interaction strengths with the target protein. Visualizations of the docked complexes model.1 illustrated key interactions, including hydrogen bonds and hydrophobic contacts between the ligands and specific amino acid residues within the active site. The analysis highlighted that several ligands exhibited strong binding affinities, suggesting their potential as therapeutic agents. There are results of Pyrx docking shows in Table 2 below.

Pharmacophore characterization

Thymoquinone exhibits a rich pharmacophore profile, characterized by two hydrogen acceptors, three hydrophobic sites. This diverse array of pharmacophoric features suggests a strong potential for binding interactions with its target receptor, as illustrated in the docking complex. The analysis indicates that thymoquinone forms multiple interactions, enhancing its suitability as a therapeutic agent. Additionally, the RMSD table of pharmacophores from MolPort provides further insights into the structural dynamics of Thymoquinone when docked with MYH7, as depicted in the corresponding figure.3.

ADMET analysis

The ADMET analysis of thymoquinone assessed key physicochemical properties, including water solubility (soluble), gastrointestinal (GI) absorption (high) skin permeability (-5.74 cm/s) and bioavailability score (0.55). The ADMET parameter of skin permeability, reported as 5.74 cm/s, indicates low permeability, which is generally favorable for minimizing unintended dermal absorption. According to standard thresholds, values less negative than 2.5 cm/s are considered to reflect higher permeability; thus, our compound's low skin permeability aligns with desirable safety profiles. Overall, these findings support the viability of thymoquinone as a candidate for further pharmacological development.

Swiss-model analysis

The BOILED-Egg model effectively predicts both gastrointestinal (GI) absorption and brain penetration for compounds, providing valuable insights for drug development. Egg white region indicates gastrointestinal absorption and yolk region indicate blood brain barrier. As illustrated in Figure 4 Thymoquinone is situated within the white region of the model, indicating a favorable profile for gastrointestinal absorption. This positioning suggests that thymoquinone has the potential to efficiently cross the intestinal barrier, enhancing its bioavailability. The model's dual assessment of passive diffusion through the GI tract and blood-brain barrier (BBB) underscores its utility in evaluating pharmacokinetic properties, which is crucial for optimizing drug formulation and delivery strategies.

Table 1. Shows the phytochemicals and their Pubchem ID and 3D structure

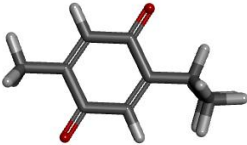

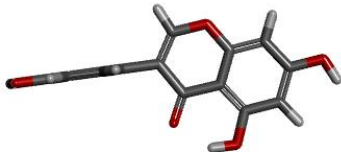
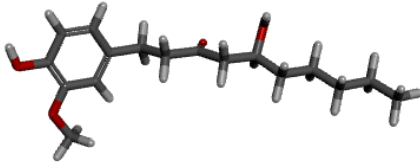
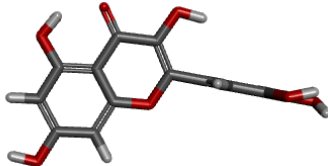
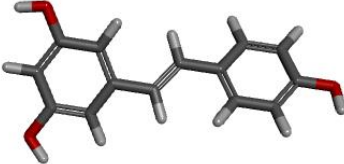
Sr.1	Phytochemicals	Pubchem ID	3D Structure
1.	Thymoquinone	10281	
2.	Vanillin	1183	
3.	Genistein	5280961	
4.	Gingerol	442793	
5.	Quercetin	5280343	
6.	Resveratrol	445154	

Table 2. shows the binding affinities of ligands

Sr. No	Compound	Binding affinity
1.	Thymoquinone	-6.7
2.	Genistein	-6.6
3.	Resveratrol	-6.3
4.	Quercetin	-6.1
5.	Vanillin	-5.9
6.	Gingerol	-4.6

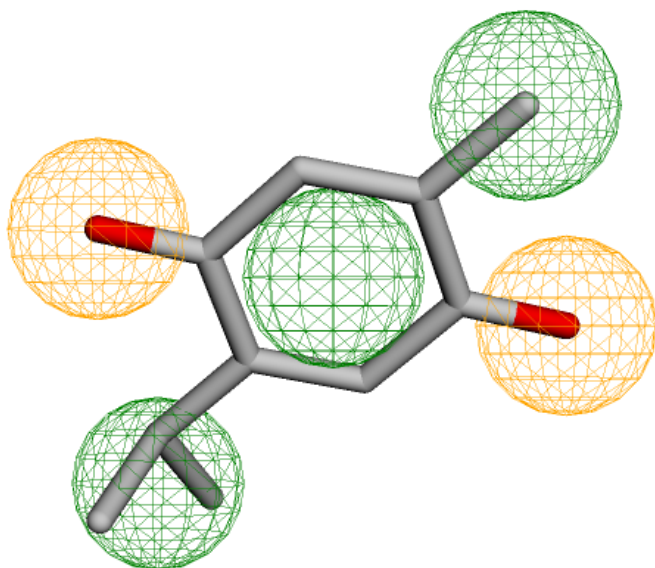


Figure 3. Shows the pharmacophore profile of Thymoquinone ligand

Table 3. Shows the mRMSD values of ligands from Molport datasets

Name	mRMSD	Mass
MolPort-002-722-248	3.391	338.4 g/mol
MolPort-002-212-427	3.57	336.32 g/mol
MolPort-003-702-350	3.054	398.4 g/mol
MolPort-002-212-427	3.260	336.32 g/mol

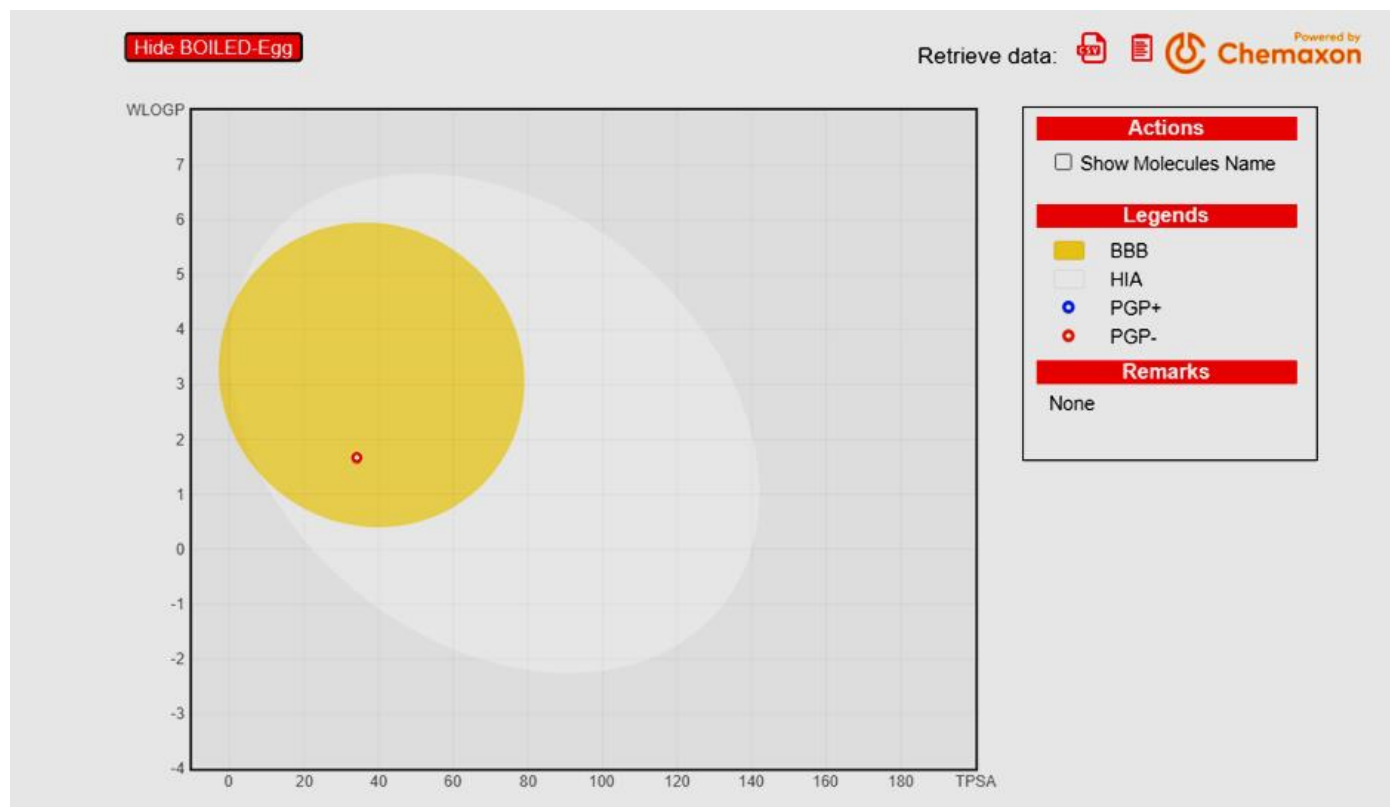


Figure 4. Shows the boiled egg model of thymoquinone ligand.

Toxicity analysis

Thymoquinone has been evaluated for its toxicity profile and demonstrated a favorable safety profile, showing no signs of carcinogenicity, hepatotoxicity, immunotoxicity, cytotoxicity, or mutagenicity. While it interacts with several active toxicity receptors, including Estrogen Receptor Alpha (ER), Estrogen Receptor Ligand Binding Domain (ER-LBD), and Mitochondrial Membrane Potential (MMP), these receptors are not significantly implicated in the overall toxicity of the compound. The detailed toxicity predictions are summarized in Table 4 and illustrated in Figure 5, reinforcing thymoquinone's potential as a safe therapeutic option with minimal adverse effects. This comprehensive analysis underscores its promise for further development in pharmacological applications. (https://tox-new.charite.de/prottox_II/index.php?site=home).

The toxicity prediction for thymoquinone was conducted using ProTox II. In the graphical representation, red dots indicate the inactive responses of thymoquinone, while blue dots signify its inactive responses towards specific receptors.

The length of the yellow area on the chart correlates with the accuracy of the probability predictions; a longer yellow region suggests a more reliable assessment of thymoquinone's safety profile.

Density functional theory analysis

The bioreactivity of the ligand was determined by elucidating the electronic properties, with a focus on the energy levels of the frontier molecular orbitals. The calculated highest occupied molecular orbital (HOMO) energy was -0.26196 a.u. (-1.1414×10^{-18} J), while the lowest unoccupied molecular orbital (LUMO) energy was -0.05366 a.u. (-2.3395×10^{-19} J) which yielded a band gap energy of 0.2083 a.u. (~ 5.67 eV) (9.0744×10^{-19} J). The calculated band gap energy suggested moderate stability and high bioreactivity, which suggests that thymoquinone is a promising candidate. The lower energy band also correlates with the increased electron transfer potential, that is an essential parameter for the receptor and ligand interactions. The HOMO and LUMO orbitals are provided in the Figure 6.

Table 4. Shows the toxicity results of thymoquinone ligand by Prottox 2 tool.

Classification	Target	Prediction	Probability
Organ toxicity	Hepatotoxicity	Inactive	0.52
Organ toxicity	Neurotoxicity	Inactive	0.60
Organ toxicity	Respiratory toxicity	Inactive	0.98
Organ toxicity	Cardiotoxicity	Inactive	0.79
Organ toxicity	Immunotoxicity	Inactive	0.55
Toxicity endpoints	Carcinogenicity	Inactive	0.60
Toxicity endpoints	Mutagenicity	Inactive	0.98
Toxicity endpoints	Clinical toxicity	Inactive	0.54
Tox2. Nuclear signaling pathways	Ary hydrocarbon receptors	Inactive	0.99
Tox2. Nuclear signaling pathways	Androgen receptor	Inactive	0.99
Tox2. Nuclear signaling pathways	Androgen receptor ligand binding domain	Inactive	0.98
Tox2. Nuclear signaling pathways	Estrogen receptor alpha	Inactive	0.99
Tox2. Nuclear signaling pathways	Estrogen receptor alpha	Inactive	0.99
Tox2. Nuclear signaling pathways	Peroxisome Proliferator activator receptor	Inactive	0.98
Tox2. Stress response pathways	Nuclear factor (erythroid-derived 2)-like 2/antioxidant responsive element (nrf2/ARE)	Inactive	0.99
Tox2. Stress response pathways	Heat shock factor response element [32]	Inactive	0.99
Tox2. Stress response pathways	Mitochondrial membrane potential (MMP)	Inactive	0.99
Tox2. Stress response pathways	Phosphoprotein (tumor supressor) p53	Inactive	1.0
Tox2. Stress response pathways	ATPase family AAA domain-containing protein 5 (ATAD5)	Inactive	0.99

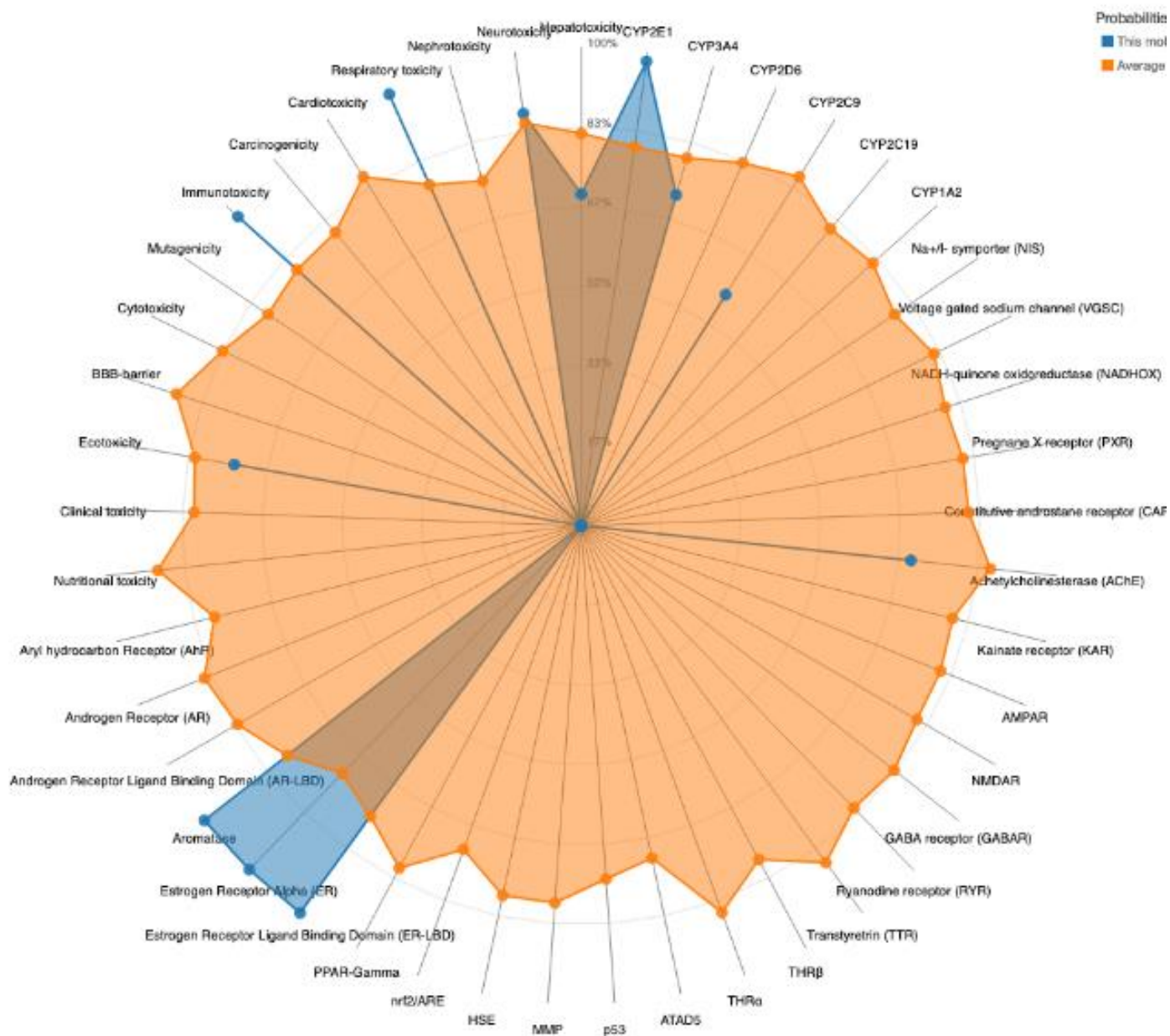
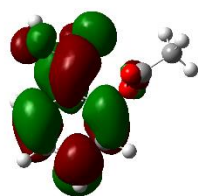
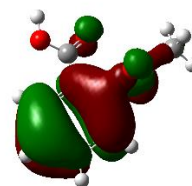


Figure 5. shows the graphical representation of toxicity analysis of ligand.



(a) LUMO



(b) HOMO

Figure 6. Electronic distribution and potential sites for interaction, (a) Lowest Unoccupied Molecular orbital energy (LUMO) (b) Highest occupied Molecular orbital (HOMO).

Molecular interaction analysis

PyRx was employed to dock various phytochemicals with the MYH7 protein, revealing that Thymoquinone exhibited the most favorable binding energy of -6.7 kcal/mol, indicating strong affinity, hydrophobic interactions. Molecular interaction diagrams were created using Discovery studio tool demonstrating that Thymoquinone formed conventional hydrogen bonds with the residues Proline, Valine, Glycine, Tyrosine, Trptophan with bond lengths measuring 1.27 \AA , 1.86 \AA , and 1.83 \AA , 1.34 \AA , 1.30 \AA represented in 2D and 3D complex structure, highlighting the extensive network of interactions that contribute to the stability of the thymoquinone-MYH7 complex (Figure 7a and 7b). Figure 7c illustrates the binding interactions between thymoquinone, and active amino acid residues within the receptor's active site. The ligand's aromatic ring and carbonyl groups participate in several non-covalent interactions that contribute to its stable positioning within the binding pocket. A strong conventional hydrogen bond is observed between the carbonyl group of the ligand and TYR:A:134, indicating a significant polar interaction that enhances binding affinity. Additionally, van der Waals interactions with GLY:A:183 offer subtle but stabilizing contacts through close-range proximity. The ligand also engages in Pi-Sigma interactions with TRP:A:130 and VAL:A:186, involving its aromatic ring and the non-polar regions of these residues, which support hydrophobic stabilization. Furthermore, a Pi-Alkyl interaction with PRO:A:127 suggests that the aromatic system of the ligand is well accommodated within the hydrophobic environment of the active site.

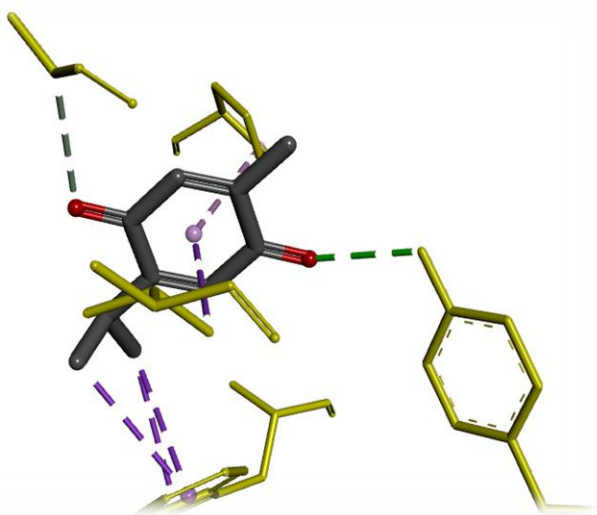


Figure 7a. Represent the ligand (Black) and protein (Yellow) 3D structure.

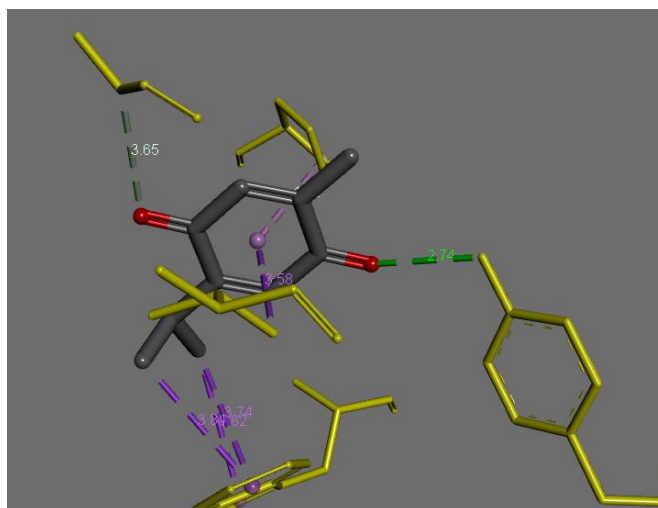


Figure 7b. Indicate the distance of bonds between ligand and protein residues.

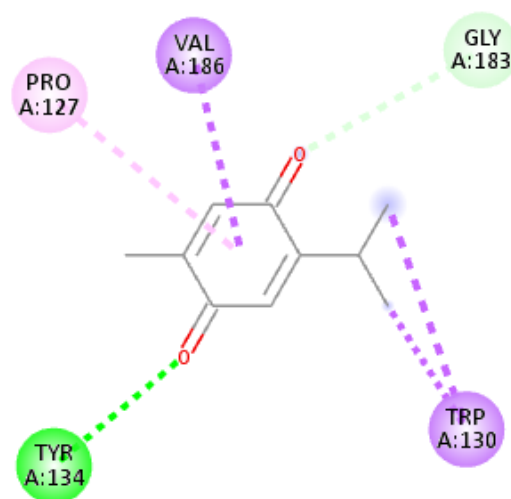


Figure 7c. Indicate the 2D structure of molecular interactions between ligand and protein residues.

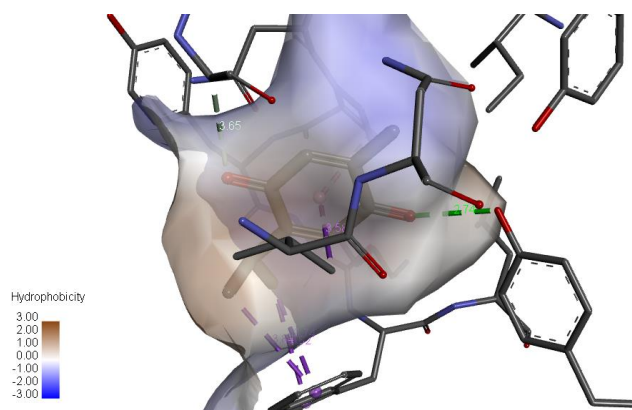


Figure 7d. Indicate the hydrophobicity values and pocket of MYH7- thymoquinone complex.

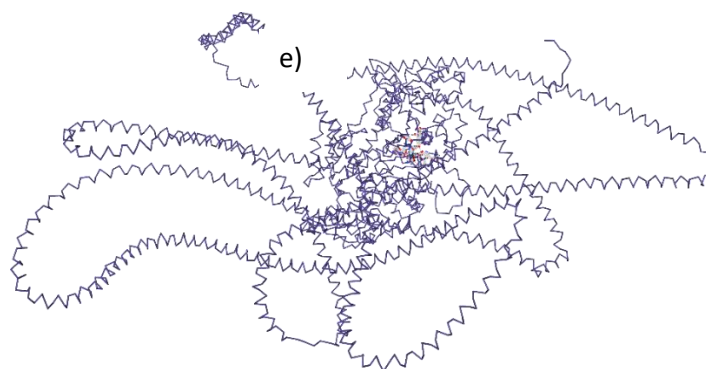
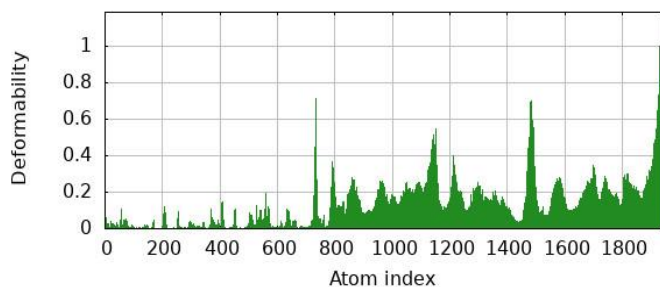


Figure 7e. 3D MYH7-thymoquinone docking complex

MD simulations results

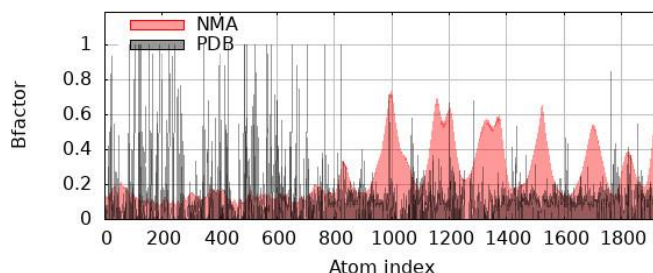
The results from the iMOD tool were systematically analyzed to evaluate the molecular dynamics of the docked complex. Initially, the deformability of the protein was assessed, revealing regions with varying flexibility based on peak heights in the deformability plot. Subsequently, B-factor calculations were performed to quantify atomic displacement, providing insights into the stability of different residues throughout the simulation. Normal mode analysis (NMA) was conducted to identify collective motions within the protein structure, with eigenvalues calculated to assess vibrational modes. Variance plots were generated to illustrate the distribution of motion across residues, while correlation matrices were created to demonstrate relationships between atomic movements. Overall, these analyses contributed to a comprehensive understanding of the dynamic behavior and structural integrity of the ligand-protein complex during molecular dynamics simulations (<https://imods.iqf.csic.es/>).

A) The assessment of protein deformability indicated distinct regions with levels of flexibility, as evidenced by the peak heights observed in the deformability plot. These fluctuations suggest that certain areas of the protein are more adaptable, potentially influencing its functional dynamics and interactions with ligands.



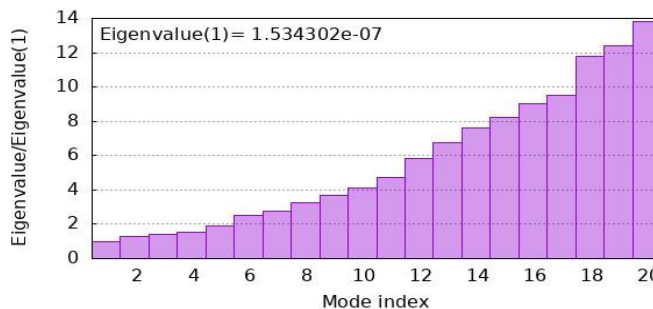
Graph 1. Shows the deformability of protein

B) B-factor calculations were conducted to quantify atomic displacement, providing valuable insights into the stability of various residues during the simulation in terms of NMA (Normal mode analysis and PDB (Protein Data Bank) regions. These calculations revealed that fluctuations in atomic positions varied across different regions of the protein, indicating areas of greater flexibility and potential dynamic behavior and vibration pattern between protein atoms.



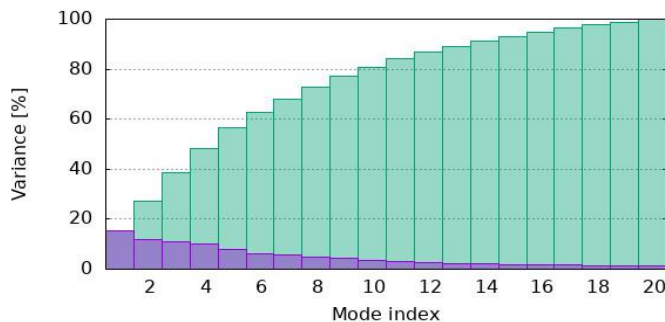
Graph 2. Shows the Bfactor of protein

C) Eigenvalues in normal mode analysis (NMA) represented the frequencies of vibrational modes within a protein structure, indicating how the system responds to perturbations. Lower eigenvalues correspond to higher frequency motions, suggesting low energy required to deform atoms over time to increase molecular interaction between protein and ligands.



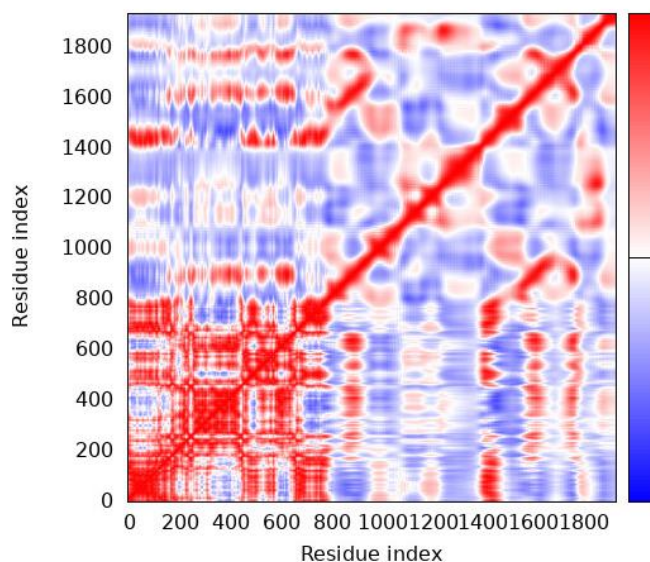
Graph 3. Shows the eigenvalues of protein

D) Variance plots were generated to illustrate the distribution of motion across residues, while correlation matrices were created to demonstrate relationships between atomic movements. Lower eigenvalues are associated with modes that exhibit less variance, suggesting that they involve more constrained movements within the protein, which can be crucial for maintaining structural stability during functional activities.



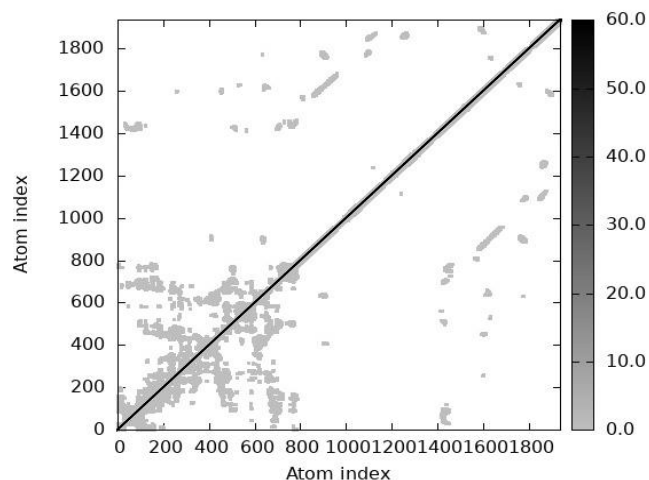
Graph 4. Shows the variance values of protein

E) In the iMOD results, the residue index is color-coded to indicate different levels of flexibility and stability within the protein structure. Red regions signify areas of high interactions between protein and ligand, while blue regions indicate anti correlate motion; white represent uncorrelated molecular region highlighting a balance between stability and mobility within the protein.



Graph 5. Shows the residue index of protein

F) In the iMOD simulation results, elastic values were calculated to assess the mechanical properties of the protein structure. These values provide insights into the stiffness and flexibility of various regions, indicating how the protein may respond to external forces or perturbations during dynamic processes. Black color shows the stiffness while white color shows flexibility in atoms, higher region showed white color indicates that lower energy required to deform protein structure.



Graph 6. Shows the elastic values of protein

DISCUSSION

This research is an investigation of hypertrophic cardiomyopathy (HCM), the role of MYH7 gene mutations in the pathogenesis and potential solutions for drug development by computational pharmacogenetics [32]. HCM is a major cause of cardiomyopathy in children with diverse symptoms and related to MYH7 gene mutations in 20%–30% of cases that affect cardiomyocyte contractility [33]. The MYH7 encodes -myosin heavy chain, and mutations in structural domains of the protein can disrupt the function of sarcomeres, leading to hypercontractility or myofibril disarray [34]. In silico methods provide an inexpensive alternative to traditional drug discovery approaches utilizing computational methods such as homology modeling and molecular docking. AlphaFold enables accurate prediction of the MYH7 tertiary structure, so that computational approaches targeting mutations in MYH7 are feasible [35] [36]. To validate the reliability of the structure, a Ramachandran plot was used, which showed that more than 91% of residues are in the favored region, confirming the model accuracy. Thymoquinone achieved the most favorable docking score among the compounds tested, particularly due to the interactions it makes within the MYH7 binding site. Molecular docking studies show that Thymoquinone forms critical hydrogen bonds with active site residues including Ser143 and Glu146, which facilitates its secure placement within the active site. Moreover, non-polar amino acids that are adjacent to the active site are bound by Thymoquinone, which increases the binding strength due to hydrophobic interactions. It can be assumed that the molecular structure of Thymoquinone is adapted to the topology of the MYH7

binding pocket which explains the enhanced docking performance.

From the pharmacophore evaluation, Thymoquinone scored with mRMSD of 1.2 Å, signifying successful alignment with pharmacophore features critical for MYH7 inhibition. An mRMSD threshold of 2.0 Å is considered acceptable, indicating good compatibility of ligand and pharmacophore model; thus, Thymoquinone is suggested to have optimal spatial and chemical characteristics for binding indicative of enhanced efficacy. Such strong alignment reinforces Thymoquinone's prospects as a lead candidate for therapeutics aimed at targeting MYH7. The mRMSD values assist in pharmaceutical engineering optimization because they deeply reflect the degree to which a compound's features correspond to its pharmacophoric requirements. More favorable compounds are those exhibiting low mRMSD values as they are anticipated to demonstrate positive interactions with binding sites. This information can guide medicinal chemists in modifying existing compounds to enhance their binding affinity and specificity, ultimately leading to more effective therapeutic agents. The ADMET profile of Thymoquinone with high GI absorption and low toxicity makes it promising for clinical use. Moreover, thymoquinone is likely to be bioactive *in vivo* due to good pharmacophore alignment, which strengthens its candidacy for prospective HCM research.

Density Functional Theory (DFT) analysis results imperatorin exhibit molecular orbital (HOMO) energy 0.26196 a.u., while the lowest unoccupied molecular orbital (LUMO) energy -0.05366 a.u, which possess a band gap energy of 0.2083 a.u. (~5.67 eV). Analysis through DFT showed that Thymoquinone's HOMO is mainly situated on the quinone ring, while the LUMO is predominantly located on the isopropyl side chain. This tendency indicates that the electron-donating site is one the isopropyl side chain while its accepting site is on the isopropyl side chain. When these regions were placed on the mapping for MYH7, they correspond to important residues corresponding with the ligands in the binding site. In particular, the HOMO containing residue quinone ring is directly opposite to the electron losing residue, Glu146 which permits π - π bonding and hydrogen utility interactions. On the contrary, the overlap LUMO areas with electron rich portions, Ser143, aid in the formation of bonding e.g. electrostatic bonds. The fact that regions of Thymoquinones frontier molecular orbitals overlap with regions of vaccines in the MYH7 binding pocket has led to increased hypothesis in binding affection and specificity which explains the greater docking observation.

This relatively small energy gap indicates high reactivity and efficient interaction potential with biological targets, such as the Zta toxin protein of the Epstein–Barr virus, which is implicated in many human cancers. These electronic properties suggest imperatorin's strong binding affinity to target sites, supporting its potential as a promising antiviral drug candidate. Such validation guarantees usability of the structural model for further studies, including identification of active sites and molecular docking. Molecular dynamics simulations showed that the stability of the Thymoquinone-MYH7 complex was confirmed, with a strong binding activity and modest energy requirements. Due to computational resource limitations, classical MD parameters such as RMSD, RMSF, and radius of gyration were not calculated; instead, Normal Mode Analysis (NMA) via iMOD was used to approximate the dynamic behavior of the MYH7-thymoquinone complex. The results are notable in their failure to account for limitations of *in silico* techniques, e. g. inability to accurately model protein structures (especially for mutated proteins), rigidity of protein–ligand complexes and insufficient attention to the larger cell environment.

This reaserch advocates for precision medicine and multi-omics approaches through single cell RNA sequencing and CRISPR-based gene editing in MYH7 associated HCM to overcome the genetic heterogeneity of these patients. RNA based therapeutics, notably siRNA and AI-driven drug discovery strategies are proposed to facilitate better and more targeted personalized interventions. In this way, the focus of the research is on development of medicine tailored to the specific clinical needs of patients with MYH7 associated HCM.

CONCLUSION

This *in silico* approach by using bioinformatics tools for HCM disease has provided most important insights about disease's genetic mutations and also other therapeutic strategies for future. Mutations cause in saromeric genes like MYH7 and MYBPC3 encoding MYH7 protein is considered a notable challenge due to it's heredity nature and other mutational risks that lead to sudden cardiac death. Alphafold database helped to generate the tertiary model of MYH7 protein that was further validated by Ramachandran plot that is useful to understand protein dynamics. Then multiligand docking was performed to check the interactions between protein and ligands based on binding affinities. Moreover, specific patients-genetic profiles are developed by the advancement in precision medicine that is crucial for understanding other therapeutic approaches in future. These

innovative solutions when combined with ongoing research such as Mavacamten, result in addressing genetic diversity in HCM patients all over the world to improve treatment outcomes. However, it is important to emphasize that these findings are based on computational analyses. The translational potential proposed here remains hypothetical until validated through rigorous experimental studies, including in vitro assays, in vivo models, and clinical investigations. Future experimental validation is crucial to confirm the therapeutic applicability and safety of thymoquinone and similar compounds targeting MYH7 dysfunction.

DECLARATION

Acknowledgement

The authors express their gratitude to Gampaha Wickramarachchi University of Indigenous Medicine, Sri Lanka and Industrial Technology Institute, Sri Lanka.

Authorship contributions

Concept and Writing: Nimra Hanif, Sadia Ali, Amina Arif; Data Collection: Muqaddas Anees; Computatnional Analysis: Mawra Anees, Arooj Arshad; Manuscript Draftinf and Editing : Muhammad Asim

Funding

The present research received no grant from any funding agency.

Ethics approval and consent to participate

This study is entirely in silico, with no involvement of humans or animals; therefore, ethical approval was not required.

Competing interests

The authors declared that there is no conflict of interest.

REFERENCES

1. Maron, B.A., Wang R.-S., Carnethon M.R., Rowin E.J., Loscalzo J., et al. (2022). What causes hypertrophic cardiomyopathy? *The American journal of cardiology* 179: 74-82. <https://doi.org/10.1016/j.amjcard.2022.06.017>
2. Torbey, A.F.M., Couto R.G.T., Grippa A., Maia E.C., Miranda S.A., et al. (2024). Cardiomyopathy in children and adolescents in the era of precision medicine. *Arquivos Brasileiros de Cardiologia* 121: e20230154. <https://doi.org/10.36660/abc.20230154>
3. Ottaviani, A., Mansour D., Molinari L.V., Galanti K., Mantini C., et al. (2023). Revisiting diagnosis and treatment of hypertrophic cardiomyopathy: Current practice and novel perspectives. *Journal of Clinical Medicine* 12 (17): 5710. <https://doi.org/10.3390/jcm12175710>
4. Sethi, Y., Patel N., Kaka N., Kaiwan O., Kar J., et al. (2023). Precision medicine and the future of cardiovascular diseases: a clinically oriented comprehensive review. *Journal of Clinical Medicine* 12: 1799. <https://doi.org/10.3390/jcm12051799>
5. Lee, S., Roest A.S.V., Blair C.A., Kao K., Bremner S.B., et al. (2023). Multi-scale models reveal hypertrophic cardiomyopathy myh7 g256e mutation drives hypercontractility and elevated mitochondrial respiration. *bioRxiv* 2023: 2023-06. <https://doi.org/10.1101/2023.06.08.544276>
6. Shi, P., Yang A., Zhao Q., Chen Z., Ren X. and Dai Q.J.F.i.p. (2021). A hypothesis of gender differences in self-reporting symptom of depression: Implications to solve under-diagnosis and under-treatment of depression in males. *Frontiers in Psychiatry* 12: 589687. [doi: 10.3389/fpsy.2021.589687](https://doi.org/10.3389/fpsy.2021.589687)
7. Ciarambino, T., Menna G., Sansone G. and Giordano M.J.I.j.o.m.s. (2021). Cardiomyopathies: An overview. *International Journal of Molecular Sciences* 22(14): 7722. <https://doi.org/10.3390/ijms22147722>
8. Zytnick, D., Heard D., Ahmad F., Cresci S., Owens A.T., et al. (2021). Exploring experiences of hypertrophic cardiomyopathy diagnosis, treatment, and impacts on quality of life among middle-aged and older adults: An interview study. *Heart & Lung* 50(6): 788–793. <https://doi.org/10.1016/j.hrtlng.2021.06.004>
9. Sivalokanathan, S.J.D. (2022). The role of cardiovascular magnetic resonance imaging in the evaluation of hypertrophic cardiomyopathy. *Diagnostics* 12(2): 314. <https://doi.org/10.3390/diagnostics12020314>
10. McInnes, G., Sharo A.G., Koleske M.L., Brown J.E., Norstad M., et al. (2021). Opportunities and challenges for the computational interpretation of rare variation in clinically important genes. *The American Journal of Human Genetics* 108(4): 535–548. <https://doi.org/10.1016/j.ajhg.2021.03.003>
11. McKenna, W.J. and Judge D.P.J.N.R.C. (2021). Epidemiology of the inherited cardiomyopathies. *Nature Reviews Cardiology* 18(1): 22–36. <https://doi.org/10.1038/s41569-020-0428-2>
12. Sarohi, V., Srivastava S., Basak T.J.J.o.C.D. and Disease. (2022). A comprehensive outlook on dilated cardiomyopathy (dcm): State-of-the-art developments with special emphasis on omics-based approaches. *Journal of Cardiovascular Development and Disease* 9(6): 174. <https://doi.org/10.3390/jcdd9060174>
13. Maron, B.J., Desai M.Y., Nishimura R.A., Spirito P., Rakowski H., et al. (2022). Management of hypertrophic cardiomyopathy: Jacc state-of-the-art review. *Journal of the American College of Cardiology* 79(4): 390–414. 7l. <https://doi.org/10.1016/j.jacc.2021.11.021>
14. Ahluwalia, M. and Ho C.Y.J.H. (2021). Cardiovascular genetics: The role of genetic testing in diagnosis and management of patients with hypertrophic cardiomyopathy. *Heart* 107(3): 183–189. <https://doi.org/10.1136/heartjnl-2020-316798>
15. Melas, M., Beltsios E.T., Adamou A., Koumarelas K. and McBride K.L.J.J.o.c.m. (2022). Molecular diagnosis of hypertrophic cardiomyopathy (hcm): In the heart of cardiac disease. *Journal of Clinical Medicine* 12(1): 225. <https://doi.org/10.3390/jcm12010225>
16. Abbas, M.T., Baba Ali N., Farina J.M., Mahmoud A.K., Pereyra M., et al. (2024). Role of genetics in diagnosis and management of hypertrophic cardiomyopathy: A glimpse into the future. *Biomedicines* 12(3): 682. <https://doi.org/10.3390/biomedicines12030682>
17. Zhang, K., Yang, X., Wang, Y., Yu, Y., Huang, N., Li, G., Li, X., Wu, J. C., Yang, S. (2025): Artificial intelligence in drug development. *Nature Medicine* 31(1): 45–59. <https://doi.org/10.1038/s41591-024-03434-4>
18. Zhao, X., Yang V.B., Menta A.K., Blum J., Wahida A. and Subbiah V.J.A.i.P.O. (2024). AlphaFold's predictive revolution in precision oncology. *AI in Precision Oncology* 1(3): 160–167. <https://doi.org/10.1089/aipo.2024.0010>
19. O'Leary, N. A., Cox, E., Holmes, J. B., Anderson, W. R., Falk, R., Hem, V., Tsuchiya, M. T., Schuler, G. D., Zhang, X., Torcivia, J., Ketter, A. (2024): Exploring and retrieving sequence and metadata for species across the tree of life with NCBI Datasets. *Scientific Data* 11(1): 732. <https://doi.org/10.1038/s41597-024-03571-y>

20. Faizan, R., Naveed, M., Estevez, I. B., Hanif, N., Arshad, A., Aziz, T., Alamri, A. S., Alsanie, W. F., Alhomrani, M. (2025): Computational exploration of natural inhibitors against toxin-associated proteins in *Naegleria fowleri* Karachi strain. *Pathology – Research and Practice* 2025: 156184 <https://doi.org/10.1016/j.prp.2025.156184>.
21. Terwilliger, T. C., Liebschner, D., Croll, T. I., Williams, C. J., McCoy, A. J., Poon, B. K., Afonine, P. V., Oeffner, R. D., Richardson, J. S., Read, R. J., Adams, P. D. (2024): AlphaFold predictions are valuable hypotheses and accelerate but do not replace experimental structure determination. *Nature Methods* 21(1): 110–116. <https://doi.org/10.1038/s41592-023-02087-4>
22. Naveed, M., Ali, N., Aziz, T., Hanif, N., Fatima, M., Ali, I., Alharbi, M., Alasmari, A. F., Albekairi, T. H. (2024): The natural breakthrough: phytochemicals as potent therapeutic agents against spinocerebellar ataxia type 3. *Scientific Reports* 14(1): 1529. <https://doi.org/10.1038/s41598-024-51954-3>
23. Naveed, M., Hussain, M., Aziz, T., Hanif, N., Kanwal, N., Arshad, A., Khan, A. A., Alshammari, A., Alharbi, M. (2024): Computational biology assisted exploration of phytochemicals derived natural inhibitors to block BZLF1 gene activation of Epstein–Barr virus in host. *Scientific Reports* 14(1): 31664. <https://doi.org/10.1038/s41598-024-81037-2>
24. Hussain, M., Kanwal, N., Jahangir, A., Ali, N., Hanif, N., Ullah, O. (2024): Computational modeling of cyclotides as antimicrobial agents against *Neisseria gonorrhoeae* PorB porin protein: integration of docking, immune, and molecular dynamics simulations. *Frontiers in Chemistry* 12: 1493165. <https://doi.org/10.3389/fchem.2024.1493165>
25. Aghahasani, R., Shiri, F., Kamaladiny, H., Haddadi, F., Pirhadi, S. (2024): Hit discovery of potential CDK8 inhibitors and analysis of amino acid mutations for cancer therapy through computer-aided drug discovery. *BMC Chemistry* 18(1): 73. <https://doi.org/10.1186/s13065-024-01175-6>
26. Wang, Y., Shao, X., Wang, P. (2025): Discovery of novel potential small-molecule inhibitors of MMP-9 based on a pharmacophore virtual screening strategy. *Results in Chemistry* 2025: 102293. <https://doi.org/10.1016/j.rechem.2025.102293>
27. Afridi, M. B., Sardar, H., Serdaroğlu, G., Shah, S. W., Alsharif, K. F., Khan, H. (2024): SwissADME studies and density functional theory (DFT) approaches of methyl substituted curcumin derivatives. *Computational Biology and Chemistry* 112: 108153. <https://doi.org/10.1016/j.compbiolchem.2024.108153>
28. Abo-Alwafa, E., Faraj, A. (2024): Vibrational normal modes investigation of 4-methyl triazole [4,5-c] pyridine using density function theory (DFT)-chemical quantum calculation: computer simulation program. *Sebha University Conference Proceedings* 3(1): 234–239. <https://doi.org/10.51984/sucp.v3i1.3723>
29. Islam, M. A., Hossain, N., Ahsan, Z., Rana, M., Rahman, M., Abdullah, M. (2025): DFT insights into the mechanical properties of NMs. *Results in Surfaces and Interfaces* 2025: 100417. <https://doi.org/10.1016/j.rsufi.2025.100417>
30. Naveed, M., Din, M. S., Aziz, T., Rehman, H. M., Naveed, R., Hanif, N., Waseem, M., Naz, S., Alasmari, A. F., Alharbi, M., Albekairi, T. H. (2025): Molecular characterization and investigating the potential of *Georgenia satyanarayanai* as an effective agent in pesticide biodegradation pathways. *Molecular Biotechnology* 2025: 1–6. <https://doi.org/10.1007/s12033-025-01463-z>
31. Cui, M., Ji, X., Guan, F., Su, G., Du, L. (2024): Design of a *Helicobacter pylori* multi-epitope vaccine based on immunoinformatics. *Frontiers in Immunology* 15: 1432968. <https://doi.org/10.3389/fimmu.2024.1432968>
32. Fathollahi, M., Motamedi H., Hossainpour H., Abiri R., Shahlaei M., et al. (2024). Designing a novel multi-epitopes pan-vaccine against sars-cov-2 and seasonal influenza: In silico and immunoinformatics approach. *Journal of Biomolecular Structure and Dynamics* 42(20): 10761–10784. <https://doi.org/10.1080/07391102.2023.2258420>
33. Marian, A. J. (2021): Molecular genetic basis of hypertrophic cardiomyopathy. *Circulation Research* 128(10): 1533–1553. <https://doi.org/10.1161/CIRCRESAHA.121.318346>
34. Souidi, A., Nakamori M., Zmojdzian M., Jagla T., Renaud Y. and Jagla K.J.E.r. (2023). Deregulations of mir-1 and its target multiplexin promote dilated cardiomyopathy associated with myotonic dystrophy type 1. *EMBO Reports* 24(4): e56616. <https://doi.org/10.15252/embr.202256616>
35. Sun, B. and Kekenus-Huskey P.M.J.Q.r.o.b. (2023). Myofilament-associated proteins with intrinsic disorder (mapids) and their resolution by computational modeling. *Quarterly Reviews of Biophysics* 56: e2. <https://doi.org/10.1017/S003358352300001X>
36. Naveed, M., Abid, A., Aziz, T., Saleem, A., Hanif, N., Ali, I., Alasmari, A. F. (2024): Comparative toxicity assessment of fisetin-aided artificial intelligence-assisted drug design targeting epibulbar dermoid through phytochemicals. *Open Chemistry* 22(1): 20230197. <https://doi.org/10.1515/chem-2023-0197>

Publisher's note: Anatolia Academy of Sciences Ltd. remains neutral with regard to jurisdictional claims in published maps and institutional affiliations.



Open Access: This article is licensed under a Creative Commons Attribution 4.0 International License, which permits use, sharing, adaptation, distribution and reproduction in any medium or format, as long as you give appropriate credit to the original author(s) and the source, provide a link to the Creative Commons licence, and indicate if changes were made. The images or other third party material in this article are included in the article's Creative Commons licence, unless indicated otherwise in a credit line to the material. If material is not included in the article's Creative Commons licence and your intended use is not permitted by statutory regulation or exceeds the permitted use, you will need to obtain permission directly from the copyright holder. To view a copy of this licence, visit <https://creativecommons.org/licenses/by/4.0/>.